DNA-Functionalized Au Nanoparticles

Living Templates for the Hierarchical Assembly of Gold Nanoparticles**

*Zhi Li, Sung-Wook Chung, Jwa-Min Nam, David S. Ginger, and Chad A. Mirkin**

Biological systems form sophisticated mesoscopic and macroscopic structures with tremendous control over the placement of nanoscopic building blocks within extended architectures. The promise of borrowing from nature's repertoire to organize inorganic materials on length scales relevant for applications in catalysis, photonics, and electronics has led to the pursuit of a variety of biotemplated and biomimetic strategies for the synthesis and assembly of nanoscale materials.[1–6] However, using such methods to independently control the organization of inorganic materials on multiple length scales has remained challenging.

Microorganisms including viruses, bacteria, and fungi, possess unique, structurally interesting motifs, and can reproduce quickly and inexpensively, which makes them attractive targets for use in directing materials synthesis. Their use in the fabrication of nanoscale materials has been dominated by studies of biomineralization processes, during which biological structures provide templates for, or even catalyze, naturally occurring as well as artificially induced reactions involving inorganic precursors.[7–15] Examples in nature of materials synthesis directed by microorganisms include the formation of iron oxides by bacteria, calcification in cyanobacteria, silica deposition in diatoms, and the formation of various other biogenic minerals by bacteria, lichen, algae, and fungi.[2,7,8] Other examples include the binding of metal ions to surface-layer proteins,[9] DNA,[10] virus protein cages,[11] or ordered protein assemblies[12] to initiate sites of nucleation for nanoparticle growth, and the synthesis of metallic nanocrystals through bioreduction of metal ions inside bacterial,[13] virus,[14] and fungal species.[15] Herein, we report a novel approach of using fungi to template the assembly of presynthesized and oligonucleotide-functionalized nanoparticles into ordered structures, thus allowing us to dynamically control the microscale structure of the resulting materials by relying on the fungi as living templates (Figure 1). Significantly, with this approach one can simultaneously control the organization and functionalization of the nanoscale building blocks by taking advantage of the preprogrammable interactions between the DNA-functionalized nanoparticles.

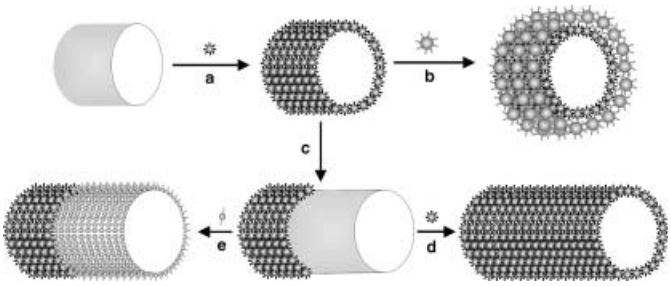

Figure 1. Schematic illustration of the use of a living hypha of a filamentous fungus as the template for the assembly of oligonucleotide-funtionalized Au nanoparticles into ordered microscopic structures. a) As the living fungal hypha grows, the Au nanoparticles (functionalized with single-stranded DNA) bind to its cell walls and a microscopic tube-shaped nanoparticle assembly is formed. b) Additional layers of nanoparticles functionalized with complementary oligonucleotide strands can be assembled onto the surface of the microscopic nanoparticle tube through DNA hybridization. c) The fungal hypha will continue to grow in a favorable environment and generate unmodified hyphae ends. d) and e) These fresh ends can be modified with new particles, thus providing control of the architecture along the growth axis.

In a typical experiment, 13-nm-diameter Au particles are prepared and modified with alkylthiol-capped oligonucleotide strands as previously reported.[16,17] On average, there are about 100 oligonucleotide strands chemically attached to each Au nanoparticle.[17] The modified Au nanoparticles are then dispersed in a culture solution (21 mM Na_2HPO_4, 11 mM KH_2PO_4, 9.3 mM NH_4Cl, 4.3 mM NaCl, 0.014 mM $CaCl_2$, 0.5 mM $MgSO_4$, 0.01 % glucose, ca. 7 nM Au particles). Subsequently, spores of a filamentous fungus, *Aspergillus niger*, are added to 20 mL of this media. Initially, this solution exhibits the characteristic intense red color of the Au nanoparticles (Figure 2a). After the fungal spores germinate, the hyphae grow and branch, while the Au nanoparticles in the media begin to assemble onto the surface of the hyphae. This results in the formation of a reddish purple macroscopic material that is phase-separated from the aqueous media and which consists of fungal mycelia heavily functionalized with nanoparticles (see below). The decrease in the red color of the media and concomitant formation of the reddish purple material can be visualized with the naked eye and have been characterized by UV/Vis spectroscopy (Figure 2b). These color changes are a direct consequence of particle assembly, which results in a red-shifting of the plasmon band associated with the gold nanoparticles—a well-documented phenomenon for other systems involving particle aggregation.[3a] Eventually, almost all of the Au nanoparticles are assembled by the fungi in the form of mycelia pellets, and the media loses its red color (Figure 2c). An optical microscope image of the mycelium fringe (Figure 2d) shows the hyphae (4–6 μm in diameter) of *Aspergillus niger*, which appear reddish purple in color.

[*] Prof. C. A. Mirkin, Z. Li, Dr. S.-W. Chung, J.-M. Nam, Dr. D. S. Ginger
Department of Chemistry and Institute for Nanotechnology
Northwestern University
2145 Sheridan Road, Evanston, IL 60208-3113 (USA)
Fax: (+1) 847-467-5123
E-mail: camirkin@chem.northwestern.edu

[**] C.A.M. acknowledges the AFOSR for financial support. In addition, this work was supported by the MRSEC program of the NSF (DMR-0076097) at the Materials Research Center of Northwestern University. Dr. W. A. Russin (BIF, Northwestern University) is acknowledged for his assistance with specimen processing and helpful discussions. In addition, we thank Dr. Y. Zhang and Prof. A. Lazarides for their valuable suggestions.

Supporting information for this article is available on the WWW under http://www.angewandte.org or from the author.

  DOI: 10.1002/ange.200351231

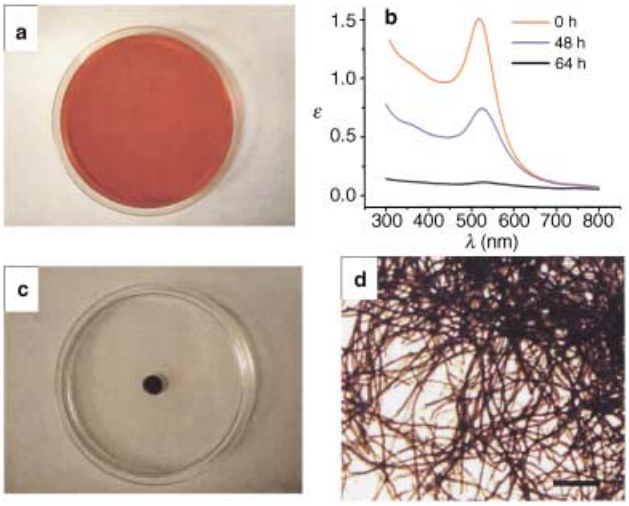

Figure 2. Au nanoparticles assembled by *Aspergillus niger*. a) Photograph of the culture media with an approximately 7 nM solution of 13-nm-diameter Au colloids immediately after introducing the fungal spores. The red color is characteristic of the Au colloid. b) UV/Vis spectra of the media during the mycelium growth process. Note that the time required for mycelia growth and nanoparticle assembly may vary from two days to more than one week. c) A reddish purple fungal mycelium is formed because of the fungal growth and Au nanoparticle assembly. Assembly of the particles onto the fungal surface depletes the solution of Au colloid. d) Optical microscope image of the fringe of the mycelium in (b). Regular branching hyphae (4–6 μm in diameter, tens of micrometers long) of *Aspergillus niger* with reddish purple color can be seen. The scale bar is 80 μm.

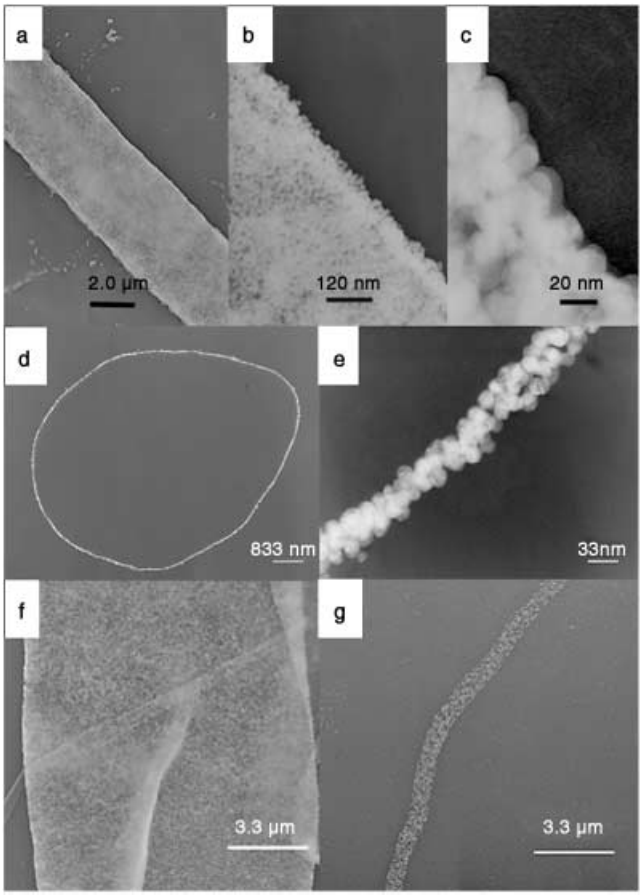

Figure 3. TEM images (unstained) of assemblies of Au nanoparticles templated by the fungal hyphae. a)–c) TEM images, at different magnifications, of the surface of an individual *Aspergillus niger* hypha heavily loaded with Au nanoparticles. d) Image of a thin section of an *Aspergillus niger* hypha loaded with Au nanoparticles embedded in epoxy resin. e) Higher magnification image of the "Au nanoparticle necklace" in (d). f) TEM image of the surface of an individual *Mucor hiemalis* hypha (ca. 12 μm in diameter) heavily loaded with Au nanoparticles. g) TEM image of the surface of an individual *Streptomyces venezuelae* hypha (ca. 0.8 μm in diameter) loaded with Au nanoparticles. Higher magnification TEM images of *Mucor hiemalis* and *Streptomyces venezuelae* hyphae in (f) and (g) are available in the Supporting Information.

Insight into the nanoparticle/fungal structure can be obtained by transmission electron microscopy (TEM). When air-dried directly on a TEM grid, the tube-shaped hyphae, loaded with nanoparticles, collapse to form thin nanoparticle-coated belt-shaped structures (Figure 3a–c). The tube shape of the nanoparticle assembly can be maintained if the mycelium is gradually dehydrated with acetone and then embedded in an epoxy resin by adding monomer to the solution and effecting thermal polymerization.[18] This was done to increase the rigidity of the material for subsequent sectioning and imaging experiments. An ultramicrotomed resin slice (approximately 80 nm thick) clearly shows that the nanoparticles assemble almost exclusively along the outer periphery of the hyphae, to form ring structures with diameters of 4–6 μm (Figure 3d). Higher magnification images show that these ring structures are made of the gold nanoparticles (Figure 3e).

When air-dried and compressed into thin films (ca. 0.2 mm), the fungal mats exhibit a golden hue and a faint metallic gloss resembling bulk gold (Figure 4a). Field emission scanning electron microscopy (FE-SEM) images show that the matted material consists of densely packed fibers with regular diameters (Figure 4b). Higher magnification TEM images show that each of these fibers derives from individual hyphae heavily functionalized with nanoparticles, which have not fused, presumably as a result of the protective oligonucleotide coating (Figure 4b; Figure 3a–c). The electrical conductivities of such films vary from 10^{-5} to 10^{-6} S cm^{-1} at room temperature, and exhibit an Arrhenius-like temperature dependence, characteristic of thermally activated charge transport between the individual Au nanoparticles (Figure 4c).[19] The semiconductive behavior and activation energy ($E_a = 1.62 \pm 0.05$ meV) of the Au-nanoparticle-assembled mycelium film are reminiscent of what has been observed for network assemblies of oligonucleotide-functionalized Au nanoparticles.[20]

Similar phenomena (nanoparticle assembly from solution and formation of fungal mats) can be observed with a variety of other common species of fungi and actinomycetes including *Penicillium notatum, Mucor hiemalis*, and *Streptomyces venezuelae*. These microorganisms grow into a range of characteristically species-dependent morphologies that allow the nanoparticles to be organized into tube-shaped structures with diameters ranging from about 12 (*Mucor hiemalis*) to 0.8 μm (*Streptomyces venezuelae*) and lengths of tens of micrometers (Figure 3f and g). At present we do not

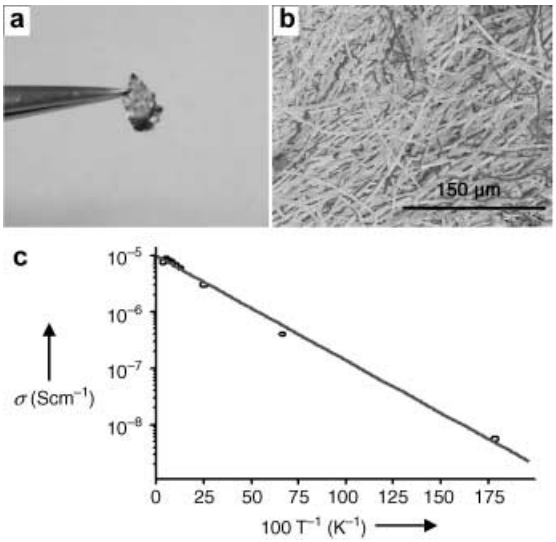

Figure 4. A thin film of gold formed from nanoparticle-fungal mycelia and its temperature-dependent electrical conductivity. a) A thin film (ca. 0.2 mm) formed by air-drying and compressing an *Aspergillus niger* mycelium loaded with oligonucleotide-functionalized 13-nm-diameter Au particles. b) FE-SEM image of the surface of the thin film in (a). Belt-shaped nanoparticle structures supported by fungal hyphae can be clearly seen. c) The electrical conductivity σ of the thin film in (a) as a function of temperature.

know the nature of the interaction between the particles and the surfaces of the fungi (for example, electrostatic versus chemical interaction). Nevertheless, the use of oligonucleotide-functionalized particles does not interfere with the assembly of the nanoparticles onto the fungal surfaces, and allows the use of sequence-specific DNA recognition properties to provide a second level of architectural control (Figure 1b).

Since the 13-nm-diameter gold particles are heavily loaded with single-stranded DNA, one can build secondary structures on the nanoscale into these micrometer-scale materials by using the sequence-specific recognition properties of their nanoparticle subcomponents. To demonstrate this capability, mycelia loaded with oligonucleotide-functionalized (5′-HS-C_6H_{12}-A_{10}AATATTGATAAGGAT-3′) 13 nm Au particles **1** were subsequently exposed to 30 nm Au particles functionalized with complementary 5′-hexylthiol-capped oligonucleotide strands (5′-HS-C_6H_{12}- A_{10}ATCCTTATCAATATT-3′). At 45 °C, the nanoparticles that make up the cottony mass hybridize with the complementary particles as evidenced by UV/Vis spectroscopy of the solution (see Supporting Information), which shows a gradual dissipation of the plasmon band (526 nm) associated with the dispersed particles, and TEM, which shows the formation of a concentric structure with two layers of different sized particles (Figure 5). Significantly, particles functionalized with DNA (30 nm, modified with 5′-hexylthiol-capped oligonucleotides, 5′-HS-C_6H_{12}- A_{10}TAACAATAATCCCTC-3′) that is noncomplementary to the 13-nm-diameter particles on the hyphae do not exhibit this behavior and remain dispersed in solution. Note that particle assembly can also be effected by using gold nanoparticles without oligonucleotide-functionalized surfaces

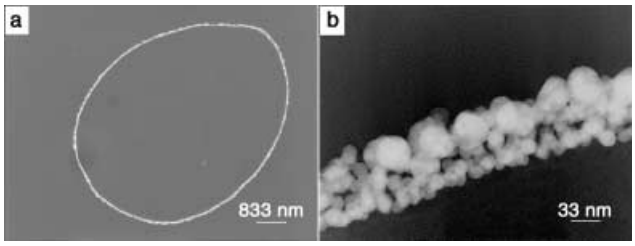

Figure 5. Double-layered nanoparticle ring structure. a) TEM image (unstained) of a thin section of an individual *Aspergillus niger* hypha, subsequently loaded with 13-nm-diameter Au particles, and then assembled with 30-nm-diameter Au particles through DNA hybridization. b) Higher magnification TEM image of the double-layered nanoparticle ring structure in (a) clearly shows the first layer of 13-nm-diameter Au particles and the second layer of 30-nm-diameter Au particles.

(for example, particles stabilized with bis(*p*-sulfonatophenyl)phenylphosphane dihydrate dipotassium salt (BSPP)). However, these particles do not allow one to control architecture through hybridization with other oligonucleotide-functionalized building blocks.

Finally, these fungal hyphae are truly living templates. Even after the dense assembly of Au particles, the mycelia will continue to grow as long as the culture media favors it (Figure 1c and d). Indeed, one can use fungal hyphae to assemble one type of particle in one solution, and then continue to assemble a second type of particle along the growing direction of the hyphae templates by changing the culture solution (Figure 1c and e). To illustrate this concept of axial arrangement of nanoparticles along the living templates as well as the living assembly process itself, an *Aspergillus niger* mycelia was first grown in the media culture containing 13-nm-diameter Au particles for about 50 h as described above, and then the surrounding solution was changed to a second culture media containing oligonucleotide-functionalized 5-nm-diameter Au nanoparticles (ca. 15 nM, only differing in particle size). After 5 h, the living assembly process was arrested when the hyphae were picked out from the growth media and air-dried onto a TEM grid (Figure 6a). As one scans along the hypha growth direction to the very end of the hypha, three different regions with different nanoparticle arrangements can be distinguished (Figure 6b–d). The region furthest from the end point of the hypha contains mainly 13-nm-diameter Au particles (Figure 6b), which assembled onto the hypha surface from the first culture media. On the other hand, only 5-nm-diameter Au particles from the second culture media can be seen in the region near the end point (Figure 6c). Between these two regions, there is a mixed region (ca. 2 μm along the hypha) containing a gradient of both 13- and 5-nm-diameter Au particles (Figure 6d; see also the Supporting Information).

In conclusion, this work provides an important example of how one can use macroscopic quantities of microorganisms as living templates to organize presynthesized nanoscale architectural components into structures with controllable micro- and nanoscale order. We anticipate that this strategy can be extended to a variety of other microorganisms, and that it could be used to construct hierarchical materials composed of

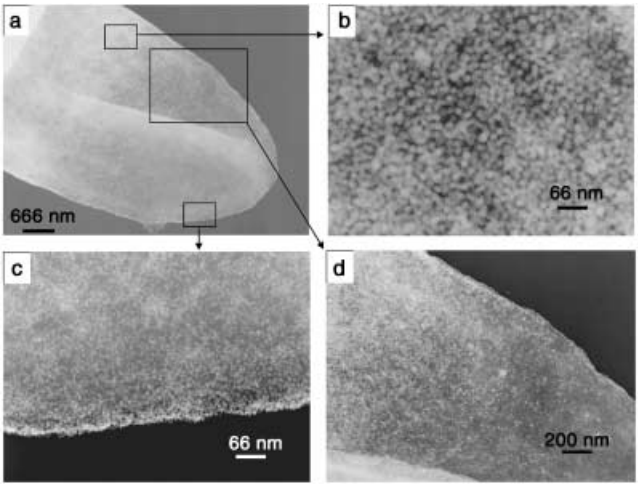

Figure 6. TEM images (unstained) of an apical growth zone of an *Aspergillus niger* hypha, grown consecutively in two culture media containing two different types of Au nanoparticles (diameters 13 nm and 5 nm, respectively), which shows the controlled distribution of these two different type of Au nanoparticles along the growth axis. a) TEM image of the whole end of the hypha, dried and captured on a carbon-coated copper grid. Three different regions with different arrangements of the nanoparticles can be distinguished as one examines sections along the hypha growth direction. b) Image of the region furthest from the apex of the hypha containing 13-nm-diameter Au paritcles. c) Image for the region closest to the apex of the hypha containing 5-nm-diameter Au paritcles. d) Transition region (ca. 2 μm along the hypha) containing a gradient of both 13- and 5-nm-diameter Au particles. Additional TEM images for (d) are available in the Supporting Information.

magnetic, semiconducting, and noble metal building blocks, thereby providing routes to high surface area macroscopic materials with novel and tailorable electronic, magnetic, optical, and catalytic properties that derive, in part, from the basic particles from which they are made.

Received: February 19, 2003 [Z51231]

Keywords: DNA · fungi · gold · nanostructures · template synthesis

[1] a) G. M. Whitesides, B. Grzybowski, *Science* **2002**, *295*, 2418 – 2421; b) M. Antonietii, C. Göltner, *Angew. Chem.* **1997**, *109*, 944 – 964; *Angew. Chem. Int. Ed. Engl.* **1997**, *36*, 910 – 928; c) C. M. Niemeyer, *Angew. Chem.* **2001**, *113*, 4254 – 4287; *Angew. Chem. Int. Ed.* **2001**, *40*, 4128 – 4158.

[2] a) S. Weiner, L. Addadi, *J. Mater. Chem.* **1997**, *7*, 689 – 702; b) S. Mann, *Biomineralization: Principles and Concepts in Bioinorganic Materials Chemistry*, Oxford University Press, Oxford, **2001**.

[3] a) C. A. Mirkin, R. L. Letsinger, R. C. Mucic, J. J. Storhoff, *Nature* **1996**, *382*, 607 – 609; b) A. P. Alivisatos, X. Peng, T. E. Wilson, K. P. Johnsson, C. J. Loweth, M. P. Bruchez, Jr., P. G. Schultz, *Nature* **1996**, *382*, 609 – 611.

[4] S. A. Davis, S. L. Burkett, N. H. Mendelson, S. Mann, *Nature* **1997**, *385*, 420 – 423.

[5] a) S.-W. Lee, C. Mao, C. Flynn, A. M. Belcher, *Science* **2002**, *296*, 892 – 895; b) Q. Wang, T. W. Lin, L. Tang, J. E. Johnson, M. G. Finn, *Angew. Chem.* **2002**, *114*, 477 – 480; *Angew. Chem. Int. Ed.* **2002**, *41*, 459 – 462.

[6] J. N. Cha, G. D. Stucky, D. E. Morse, T. J. Deming, *Nature* **2002**, *403*, 289 – 292.

[7] *Biomineralization in Lower Plants and Animals* (Eds.: B. S. C. Leadbeater, R. Riding), Clarendon Press, Oxford, **1986**.

[8] J. F. Banfield, S. A. Welch, H. Zhang, T. T. Ebert, R. L. Penn, *Science* **2000**, *289*, 751 – 754.

[9] W. Shenton, D. Pum,, U. B. Sleytr, S. Mann, *Nature* **1997**, *389*, 585 – 587.

[10] E. Braun, Y. Eichen, U. Sivan, G. Ben-Yoseph, *Nature* **1998**, *391*, 775 – 778.

[11] T. Douglas, M. Young, *Nature* **1998**, *393*, 152 – 155.

[12] S. Behrens, K. Rahn, W. Habicht, K.-J. Böhm, H. Rösner, E. Dinjus, E. Unger, *Adv. Mater.* **2002**, *14*, 1621 – 1625.

[13] T. Klaus, R. Joerger, E. Olsson, C.-G. Granqvist, *Proc. Natl. Acad. Sci. USA* **1999**, *96*, 13611 – 13614.

[14] E. Dujardin, C. Peet, G. Stubbs, J. N. Culver, S. Mann, *Nano Lett.* **2003**, *3*, 275 – 277

[15] a) P. Mukherjee, A. Ahmad, D. Mandal, S. Senapati, S. R. Sainkar, M. I. Khan, R. Ramani, R. Parischa, P. V. Ajayakumar, M. Alam, M. Sastry, R. Kumar, *Angew. Chem.* **2001**, *113*, 3697 – 3701; *Angew. Chem. Int. Ed.* **2001**, *40*, 3585 – 3588; b) P. Mukherjee, S. Senapati, D. Mandal, M. I. Khan, R. Kumar, M. Sastry, *ChemBioChem* **2002**, *3*, 461 – 463.

[16] J. J. Storhoff, R. Elghanian, R. C. Mucic, C. A. Mirkin, R. L. Letsinger, *J. Am. Chem. Soc.* **1998**, *120*, 1959 – 1964.

[17] Z. Li, R. Jin, C. A. Mirkin, R. L. Letsinger, *Nucleic Acids Res.* **2002**, *30*, 1558 – 1562.

[18] W. A. Russin, C. L. Trivett in *Microwave Techniques and Protocols* (Eds.: R. T. Giberson, R. S. Demaree, Jr.), Humana Press, Totowa, NJ, **2001**, pp. 25 – 35.

[19] M. Brust, D. Bethell, D. J. Schiffrin, C. J. Kiely, *Adv. Mater.* **1995**, *7*, 795 – 797.

[20] S.-J. Park, A. A. Lazarides, C. A. Mirkin, P W. Brazis, C. R. Kannewurf, R. L. Letsinger, *Angew. Chem.* **2000**, *112*, 4003 – 4006; *Angew. Chem. Int. Ed.* **2000**, *39*, 3845 – 3848.

